Integrative Multi-Omics Reveal Silymarin Alleviates Heat-Stress-Driven Hepatic Lipid Disruption in Laying Hens

Jiang Gao , Hongrui Ren , Xuanfu Wu , Cunzhi Zou , Bin He , Wenqiang Ma *

Posted Date: 27 February 2026

doi: 10.20944/preprints202602.1852.v1

Keywords: silymarin; heat stress; laying hen; antioxidant; liver lipid metabolism

 doi:10.20944/preprints202602.1852.v1

Article

Integrative Multi-Omics Reveal Silymarin Alleviates Heat-Stress-Driven Hepatic Lipid Disruption in Laying Hens

Jiang Gao [1,2], Hongrui Ren [1,2], Xuanfu Wu [1,2], Cunzhi Zou [1,2], Bin He [1,2] and Wenqiang Ma [1,2,*]

[1] Key Laboratory of Animal Physiology and Biochemistry, Ministry of Agriculture and Rural Affairs, College of Veterinary Medicine, Nanjing Agricultural University, Nanjing, Jiangsu 210095, China

[2] MOE Joint International Research Laboratory of Animal Health & Food Safety, Nanjing Agricultural University, Nanjing, Jiangsu 210095, China

* Correspondence: wq8110@njau.edu.cn

Abstract

Heat stress (HS) has emerged as a major environmental stressor, inducing oxidative stress, hepatic steatosis and impairing production performance and health in laying hens, with limited evidence-based nutritional interventions available. This study investigated the hepatoprotective effects of dietary silymarin (SIL) against chronic HS. In a 10-week trial, 252 43-week-old Hy-Line Brown hens were exposed to daily HS (32 ± 1°C, temperature-humidity index [THI] > 73) and fed either a basal diet or one supplemented with 100 mg/kg SIL. SIL significantly increased laying rate ($P < 0.05$) and improved albumen height, Haugh units, and shell strength by week 8 ($P < 0.05$). Histological analysis showed a 48% reduction in non-alcoholic fatty liver disease (NAFLD) activity score, with significantly decreased hepatic triglyceride content ($P < 0.05$); Oil Red O staining confirmed reduced lipid droplet accumulation. SIL restored redox balance by increasing plasma and hepatic total superoxide dismutase (T-SOD), glutathione peroxidase (GSH-Px) ($P < 0.05$), increasing hepatic catalase (CAT) and glutathione (GSH) levels while decreasing malondialdehyde (MDA) ($P < 0.05$). Untargeted plasma metabolomics identified 11 key metabolites related to 2-oxoglutarate and purine metabolism, while hepatic transcriptomics revealed 835 differentially expressed genes primarily in the PPAR signaling and fatty acid biosynthesis pathways. SIL suppressed *de novo* lipogenesis via downregulation of ACACA and FASN, and enhanced β-oxidation through upregulation of CPT1A and ACSL1 ($P < 0.05$). Molecular docking and Western blotting confirmed strong SIL binding to these targets and corresponding protein changes. Correlation networks associated ACSL1 and CPT1A with improved performance and antioxidant indices, while FASN, ACACA, and xanthosine showed inverse relationships. These findings emphasize the potential of SIL as a sustainable animal nutrition antioxidant additive, which can alleviate HS induced lipid disorders in the liver of laying hens and provide insights for livestock applications.

Keywords: silymarin; heat stress; laying hen; antioxidant; liver lipid metabolism

1. Introduction

Climate change has intensified heat-stress episodes, posing a major bottleneck for sustainable poultry production [1]. This results in economic losses exceeding billions of dollars annually from reduced productivity, morbidity, and mortality [2]. Among avian species, laying hens exhibit pronounced susceptibility owing to their elevated endogenous heat production, limited capacity for active evaporative thermoregulation, and the metabolic imperative of persistent oogenesis. Acute or chronic heat stress curtails feed intake by 15 ~ 30% and depresses productivity by 20 ~ 40%, while simultaneously derailing calcium and energy homeostasis and provoking oxidative damage, ultimately precipitating marked declines in laying performance and egg quality [3]. The hepatic

 doi:10.20944/preprints202602.1852.v1

organ serves as the primary locus mediating heat-stress-induced metabolic dysregulation [4]. Hepatocytes integrate gluconeogenic, lipid-metabolic, vitellogenic, and xenobiotic-detoxification pathways that are indispensable for ovarian follicular maturation and the biosynthesis of egg constituents [5]. Heat stress initiates hepatic steatosis, mitochondrial bioenergetic failure, and inflammatory infiltrates, which collectively compromise vitellogenin biosynthesis, yolk-precursor trafficking, and systemic metabolic efficacy [6]. Given the liver's central role, interventions targeting metabolic stability are essential - yet conventional approaches fall short.

Conventional ameliorative strategies demonstrate restricted efficacy in comprehensively mitigating heat-stress-associated pathophysiological insults [7]. These approaches often fail to maintain productivity when ambient temperatures exceed 32℃, where physiological disturbances become severe and conventional interventions reach their limits [8]. Moreover, their deployment necessitates considerable capital expenditure in infrastructure and technology, thereby presenting formidable economic barriers for smallholder or resource-limited poultry enterprises. Specifically, strategies that enhance hepatic antioxidant defense, minimize inflammation, and stabilize metabolic pathways hold promise for mitigating heat stress impacts on laying hens [9]. While pharmacological antioxidants such as vitamin E and N-acetylcysteine have been explored, their limited bioavailability and weak membrane penetration reduce their efficacy, studies show that supplementing vitamin E at 250 mg/kg diet reduces oxidative stress markers by only 20～30% under heat stress conditions, which is insufficient to prevent hepatic lipid peroxidation and mitochondrial dysfunction [10,11]. Additionally, synthetic additives face growing regulatory restrictions and consumer preference for natural alternatives. This highlights a significant research gap: the development of natural, hepatoprotective compounds capable of addressing the multifaceted challenges of heat stress in poultry. This necessitates novel, natural hepato protectants targeting redox-sensitive heat stress pathways.

Silymarin, a standardized flavonolignan complex derived from milk thistle seeds, has attracted increasing attention owing to its potent hepatoprotective, anti-inflammatory and lipid-regulating properties [12]. Silymarin effectively neutralizes reactive oxygen species (ROS), including hydroxyl and peroxyl radicals, and concurrently augments endogenous antioxidant defenses by upregulating SOD, CAT, and GSH-Px [13]. These antioxidant mechanisms are crucial for mitigating oxidative stress-induced liver damage, particularly in conditions such as NAFLD and drug-induced hepatotoxicity [14]. Beyond its antioxidant capacity, silymarin exerts profound regulatory effects on hepatic lipid metabolism. It suppresses de novo lipogenesis by downregulating sterol regulatory element-binding protein 1c (SREBP-1c) and its downstream targets, including fatty acid synthase (FAS) and acetyl-CoA carboxylase (ACC), thereby reducing triglycerides (TG) accumulation [15]. Silymarin additionally alleviates hepatic steatosis by enhancing the secretion of very-low-density lipoprotein (VLDL) through the upregulation of microsomal triglyceride transfer protein (MTTP) expression [15,16]. Importantly, silymarin exhibits an excellent safety margin, its dual antioxidant and lipid-regulating actions position it as a promising candidate. This could enhance resilience in smallholder systems, supporting UN Sustainable Development Goals amid rising temperatures.

In this study, we aimed to delineate the mechanisms by which dietary silymarin alleviates heat stress-induced hepatic lipid metabolism disorder in laying hens. We attempted to establish a causal relationship between SIL mediated steady-state improvement in laying hens by integrating performance parameters, egg quality index, plasma metabolomics, and liver transcriptomics. These findings will not only expand our understanding of liver protection mechanisms based on natural extracts in poultry, but also provide a practical, cost-effective nutritional strategy to enhance poultry resilience to face severe climate change.

 doi:10.20944/preprints202602.1852.v1

2. Materials and Methods

2.1. Breeding and Management of Animals

Two hundred and fifty-two healthy Hy-Line Brown laying hens (43 weeks of age) exhibiting uniform peak-lay productivity were randomly assigned to two dietary treatments, 126 per treatment, with six replicate pens (21 hens per pen), every 7 laying hens form an independent cage. A controlled heat-stress (HS) regimen was applied daily from 07:00 to 15:00, maintaining ambient temperature at 32 ± 1°C and relative humidity at 65 ± 5%, yielding a temperature–humidity index that clearly exceeds the established thermoneutral threshold (THI = 73) for laying hens. The control group received basal diet while experimental groups were supplemented with silymarin (98% purity) at graded levels of 100 mg/kg feed, which was received from Xi An DF Bio-Technique Co., Ltd. The 10-week study comprised a 2-week acclimation phase followed by an 8-week experimental phase. Throughout, birds were exposed to a 16L:8D photoperiod and provided water ad libitum, daily feed allocation was restricted to 130 g/bird to minimise feed refusal artefacts. Daily records were maintained for egg production rates (%) and egg weight (g), with egg quality assessments conducted at 4-week intervals. The animal experiments were approved by the Institutional Animal Care and Use Committee of Nanjing Agricultural University (Approval Number: NJAULLSC2024062). Details regarding the composition and nutritional specifications of the basal diet are presented in Table S1.

2.2. Egg Quality

Egg quality indices were assessed at 4-week intervals using a representative subsample of 50 eggs per group. Measured variables included shell mass (g) and its percentage of total egg weight, yolk weight (g) and yolk ratio (%), albumen weight (g) and albumen ratio (%), albumen height (mm), yolk colour score, Haugh unit, eggshell strength (kg/cm^2), and eggshell thickness (mm). Fracture resistance was quantified with an impact tester (Model WW-2A, Nanjing Soil Instrument Factory, China) operated at a constant loading rate until shell failure. Shell thickness was measured at three equidistant points, using a precision micrometer (0.01 mm resolution), the mean of the three readings, excluding the inner and outer shell membranes, was reported. Remaining traits were determined non-destructively by near-infrared analysis with a multifunctional egg analyser (EMT-5200, Robotmation Co., Tokyo) calibrated daily against reference standards. All measurements were performed in triplicate per egg under controlled ambient conditions (25°C, 60 ± 5% relative humidity).

2.3. Sample Collection

After analyzing laying rate and egg quality, we picked ten hens from each treatment—control and 100 mg/kg SIL—taking them evenly from the six pens for tissue and blood collection. Blood was obtained by brachial venipuncture, transferred to serum tubes (no anticoagulant), and immediately centrifuged (3,000 × g, 10 min, 4°C); plasma samples were immediately snap-frozen on ice. Segments of liver were excised and rinsed in ice-cold 0.9% saline solution. Tissue samples were then divided into two portions: one was fixed in 4% paraformaldehyde at 4°C for 24 hours for histological analysis, and the other was rapidly frozen in liquid nitrogen and stored at -80°C for subsequent molecular and biochemical assays.

2.4. Plasma Biochemistry and Metabolomics

Plasma metabolic profiles total cholesterol (TC), triglycerides (TG), high-density lipoprotein-cholesterol (HDL-C), low-density lipoprotein-cholesterol (LDL-C), alanine aminotransferase (ALT) and aspartate aminotransferase (AST) were quantified on a Hitachi 7020 automated chemistry analyser (Tokyo, Japan) using reagents supplied by Sanhe Biotechnology (Nanjing, China). Oxidative status was evaluated by spectrophotometric determination of T-SOD, MDA, GSH-Px and reduced GSH employing commercial kits (Nanjing Jiancheng Bioengineering Institute, China).

 doi:10.20944/preprints202602.1852.v1

Transcriptomic profiling of plasma samples was undertaken by Biotree Biomedical Technology Co., Ltd. (Shanghai, China). For this procedure, 100 μL of plasma was subjected to extraction with 400 μL of ice-cold methanol/acetonitrile/water (in a 2:2:1 ratio by volume), which was fortified with 2-chloro-L-phenylalanine to facilitate the process. After centrifugation (15,000 × g, 4°C, 15 min), supernatants were analysed by UPLC-HSS-T3 (0.1% formic acid gradient) coupled to a Q-Exactive HF-X Orbitrap operated at 35 000 resolutions in positive/negative modes. Peaks were processed in XCMS, annotated against HMDB (≦5 ppm) and confirmed by MS2 matching. Multivariate and pathway analyses (MetaboAnalyst 6.0) were performed with FDR < 0.05.

Liver Lipid Content and Antioxidant Activity

The hepatosomatic index was derived from aseptically excised liver mass relative to fasted body weight. Hepatic TG, TC, free cholesterol (FC) and cholesterol ester (CE) (CE = TC − FC) were quantified colorimetrically using commercial kits (TG, A110-1-1; TC, E1016-105; FC, E1015-105) in ice-cold 0.9% saline homogenates (10% w/v). Antioxidant capacity was gauged via T-SOD, GSH-Px, GSH and MDA contents using validated reagents (Nanjing Jiancheng Bioengineering Institute, China). For histology, 4% paraformaldehyde-fixed liver were paraffin-embedded and sectioned. Haematoxylin–eosin (HE) and Oil Red O staining were employed to visualise steatosis and lipid deposition; lesions were quantified using the NAFLD Activity Score (NAS) (steatosis 0-3, inflammation 0-3, ballooning 0-2) by a blinded pathologist.

2.5. Liver Transcriptomics

Liver specimens were processed for transcriptomic profiling by Biotree Biomedical Technology Co., Ltd (Shanghai, China). Hepatic transcriptome profiling was performed on 30 mg liver fragments cryo-preserved in liquid nitrogen. Total RNA was isolated with TRIzol™ reagent, treated with DNase I (Qiagen), and quantified on a NanoDrop™ One spectrophotometer (Thermo Fisher). RNA integrity (RIN ≧ 7.8) was verified by Agilent 2100 Bioanalyzer. Strand-specific libraries were constructed using the TruSeq® Stranded mRNA kit (Illumina) and sequenced on a NovaSeqTM 6000 platform with a 2 × 150 bp conFigureuration. Subsequent bioinformatics processing involved read cleaning using fastp version 0.23, alignment to the Gallus gallus GRCg6a genome assembly via HISAT2 version 2.2.1, and quantification of aligned reads with featureCounts version 2.0.3.

2.6. Quantitative Polymerase Chain Reaction

RNA was isolated from tissue homogenates with TRIzol reagent (Thermo Fisher, #15596018), followed by DNase I (Qiagen, #79254) digestion to eliminate genomic DNA. Purity was confirmed by NanoDrop 2000 (A260/280 > 1.9) and agarose electrophoresis. First-strand cDNA was synthesised from 1 μg RNA using PrimeScript RT Master Mix (Takara, #RR036A) at 37°C for 15 min and 85°C for 5 s. Gene-specific primers (see Supplementary Table S2) were designed using NCBI Primer-BLAST to produce amplicons of 90–150 bp with a melting temperature of 60 ± 2°C. Primer specificity was confirmed through melt-curve analysis, which showed a single peak within ± 0.5°C, and further validated by gel electrophoresis. Quantitative PCR was performed in 10 μL reactions containing PowerUp SYBR Green Master Mix (Applied Biosystems, #A25742), 0.5 μM of each primer, and 20 ng cDNA on a QuantStudio 6 Pro (Applied Biosystems) with UDG activation (50°C, 2 min), initial denaturation (95°C, 2 min) and 40 cycles (95°C, 15 s; 60°C, 1 min). No-template controls and inter-plate calibrators were included for each plate. Relative gene expression was calculated by the 2-ΔΔCt method, normalised to the geometric mean of β-actin and GAPDH. Primer efficiencies (90 ~ 110 %) were determined from 10-fold serial dilutions (R^2 > 0.99). Statistical analysis employed one-way ANOVA with Tukey's post-hoc test (GraphPad Prism 9.0). Each biological replicate (n = 6) was analysed in triplicate; intra- and inter-assay CVs were below 5% and 12%, respectively.

 doi:10.20944/preprints202602.1852.v1

2.7. Molecular Docking

Two dimensional and three-dimensional structures of silymarin were retrieved from PubChem and imported into ChemBio3D for energy minimisation; the resulting conformers were saved in SDF format. The crystal structure of the target protein was obtained from the RCSB PDB and AlphaFold3, and crystallographic waters were removed in PyMOL via command-line editing. Receptor and ligand were prepared with AutoDock Tools to assign rotatable bonds and partial charges, then exported as PDB files. Docking simulations were performed with AutoDock Vina; the lowest binding-energy pose was selected and visualised as a composite ligand–protein complex in PyMOL.

2.8. Western Blot

Hepatic protein extracts were prepared using ice-cold RIPA buffer (P0013B, Beyotime), supplemented with protease and phosphatase inhibitor cocktails (HY-K0010, MCE). Protein concentrations were determined by BCA assay (PC0020, Solarbio), calibrated against BSA standards. Aliquots of 50 μg were separated under reducing conditions on 6% and 10% SDS-PAGE gels (GF1800-6, GF1800-10, Genefist) at 120 V for 90 minutes, then transferred to 0.45 μm PVDF membranes via wet transfer. After blocking with 5% non-fat milk for 1 hour, membranes were incubated overnight at 4°C with primary antibodies (Table S3), washed three times with TBST, and incubated with HRP-conjugated goat anti-rabbit IgG (1:5000, Abcam, ab6721) for 2 hours at room temperature. Chemiluminescent signals were detected using ECL Basic Plus (RM00020P, Abclonal) and imaged with an Amersham Imager 600. Band intensities were quantified using ImageJ 1.53k, normalized to β-actin, and expressed as fold-changes relative to untreated controls.

2.9. Statistical Analysis

All statistical analyses were performed using SPSS Statistics 25.0 (IBM Corp., USA) and GraphPad Prism 9.0. Data are presented as mean ± standard error of the mean (SEM). For phenotypic and biochemical data, comparisons between two groups were conducted using two-tailed Student's t-tests. A two-tailed P value < 0.05 was considered statistically significant.

For omics datasets (transcriptomics and metabolomics), to control for false discovery due to multiple testing, the Benjamini - Hochberg false discovery rate (FDR) correction was applied, and only features with FDR-adjusted $P < 0.05$ were considered statistically significant. Principal component analysis (PCA) and pathway enrichment analyses were conducted using MetaboAnalyst 6.0 and clusterProfiler in R, respectively, with FDR correction applied to enriched pathways.

3. Results

3.1. Silymarin Enhances Laying Rate and Egg Quality of Laying Hens Under Heat Stress

Throughout the experimental period, the temperature–humidity index consistently exceeded 73, confirming the establishment of a robust heat-stress model (Figure 1A). Dietary silymarin significantly mitigated HS-induced losses, elevating laying rate (Figure 1B) and gradually improve the weight of eggs relative to the unsupplemented control. Part of the egg quality has a time effect, with a significant increase in albumen height and haugh units in the last four weeks (Figure 1E-F). Egg yolk color significantly increases with the feeding of silymarin (Figure 1G), and the eggshell strength of the SIL group significantly increases in the first four weeks (Figure 1K), while egg yolk weight shows a significant decrease during the feeding stage (Figure 1H).

 doi:10.20944/preprints202602.1852.v1

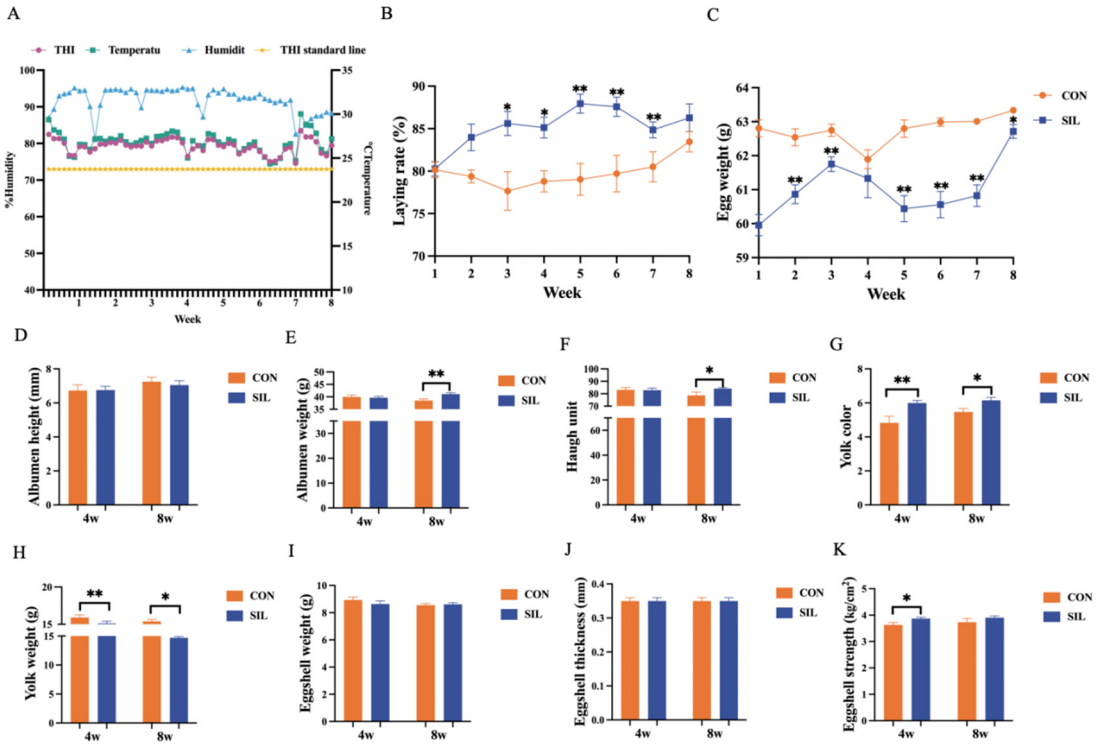

Figure 1. Effect of silymarin on laying rate and egg quality of laying hens under heat stress. **(A)** Temperature and humidity index curve. **(B)** Effects of silymarin on laying rate and **(C)** egg weight, **(D)** albumen height, **(E)** albumen weight, **(F)** haugh unit, **(G)** yolk color, **(H)** yolk weight, **(I)** eggshell weight, **(J)** eggshell thickness, **(K)** eggshell strength. Data are presented as mean ± SEM, B-C, n=6; D-K, n=25. The *P* value is calculated by student t test and two-tailed. Data are presented as mean ± SEM, n=6. * $P<0.05$, ** $P<0.01$.

3.2. Silymarin Alleviates Hepatic Steatosis in Laying Hens Under Heat Stress

Livers from control hens exhibited a yellowish, greasy surface indicative of severe steatosis (Figure 2A), whereas those from the silymarin group retained a normal bright-red appearance (Figure 2B). Histopathological assessment via HE staining revealed markedly fewer cytoplasmic vacuoles and a concomitant reduction in NAS Score (Figure 2E-G), confirming attenuated hepatic lipid accumulation. Oil Red O staining corroborated a pronounced decrease in lipid droplet density (Figure 2H). Hepatic TG and FC concentrations were significantly diminished (Figure 2I-K), whereas CE content was elevated (Figure 2L). Plasma TG and ALT activities were concurrently decreased (Figure 2N-O), while HDL-C levels and the aspartate aminotransferase/alanine aminotransferase ratio (AST/ALT) were elevated. Collectively, dietary silymarin effectively mitigated heat-stress-induced hepatic steatosis and ameliorated associated hepatic injury in laying hens.

 doi:10.20944/preprints202602.1852.v1

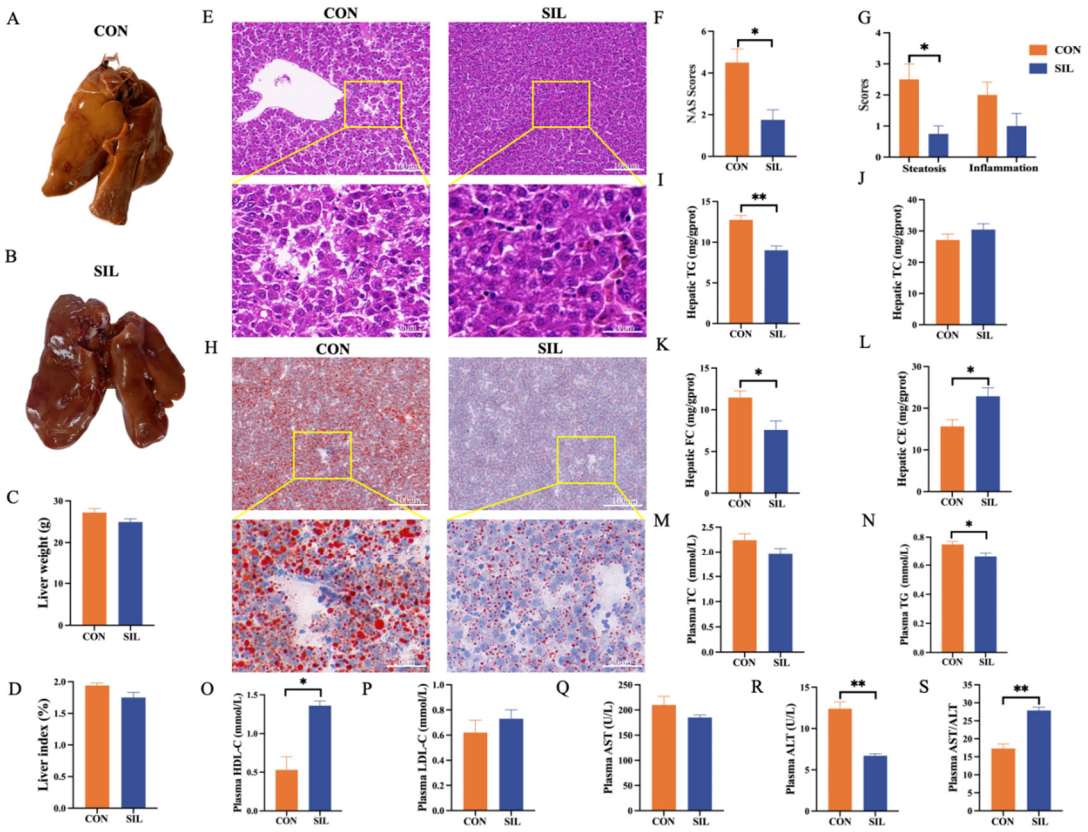

Figure 2. Effect of silymarin on liver lipid metabolism in laying hens under heat stress. **(A-B)** Gross morphology of the liver. **(C-D)** Liver weight and index. **(E)** H&E-stained sections of the liver. **(F)** NAS Score. **(G)** Histological scores for steatosis and inflammation. **(H)** Oil Red O-stained sections of the liver. **(I-L)** Hepatic lipid levels. **(M-P)** Plasma lipid levels. **(Q-S)** Liver injury indicators. The *P* value is calculated by student t test and two-tailed. Data are presented as mean ± SEM, n=6. * $P<0.05$, ** $P<0.01$.

3.3. Silymarin Enhances the Antioxidant Capacity of Laying Hens

Eight weeks of dietary silymarin elevated both plasma and hepatic T-SOD and GSH-Px activities while boosting hepatic GSH reserves (Figure 3B, 3D and 3F-H), this antioxidant reinforcement coincided with a marked decline in hepatic MDA (Figure 3E), indicating reduced oxidative injury and improved liver health in heat-stressed laying hens.

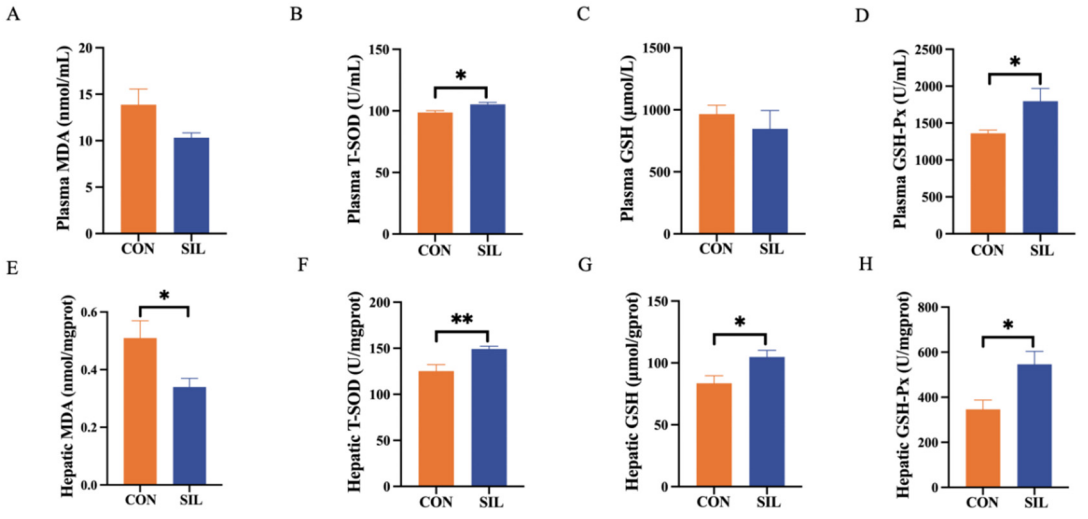

 doi:10.20944/preprints202602.1852.v1

Figure 3. Effects of silymarin on antioxidant capacity in heat stressed laying hens. **(A)** Effect of silymarin on plasma MDA and **(B)** plasma T-SOD, **(C)** plasma GSH, **(D)** plasma GSH-Px, **(E)** Effect of silymarin on hepatic MDA and **(F)** hepatic T-SOD, **(G)** hepatic GSH, **(H)** hepatic GSH-Px. The *P* value is calculated by student t test and two-tailed. Data are presented as mean ± SEM, n=6. * $P<0.05$, ** $P<0.01$.

3.4. Silymarin Alters Plasma Metabolites

Principal component analysis (PCA) exhibited a marked distinction between the two groups (Figure 4A). Significantly different metabolites were identified using a fold-change (FC) threshold of either greater than 2 or less than 0.5, with a significance level of $P < 0.01$, we identified eleven differential metabolites, three were up-regulated: S-sulfocysteine, 4-hydroxybutyric acid, and 2-oxoglutaric acid, eight were down-regulated: L-tryptophan, hydroxypropionic acid, L-glutamic acid, L-proline, aminoadipate, 1,4-butanediamine, deoxyguanosine diphosphate, and xanthosine (Figure 4B-D). Pathway enrichment indicated that these metabolites are mainly involved in 2-oxocarboxylic acid metabolism, purine metabolism, carbon metabolism, and amino-acid metabolism (Figure 4E), with 2-oxoglutaric acid serving as a central hub and 2-oxocarboxylic acid metabolism as the most affected pathway (Figure 4F).

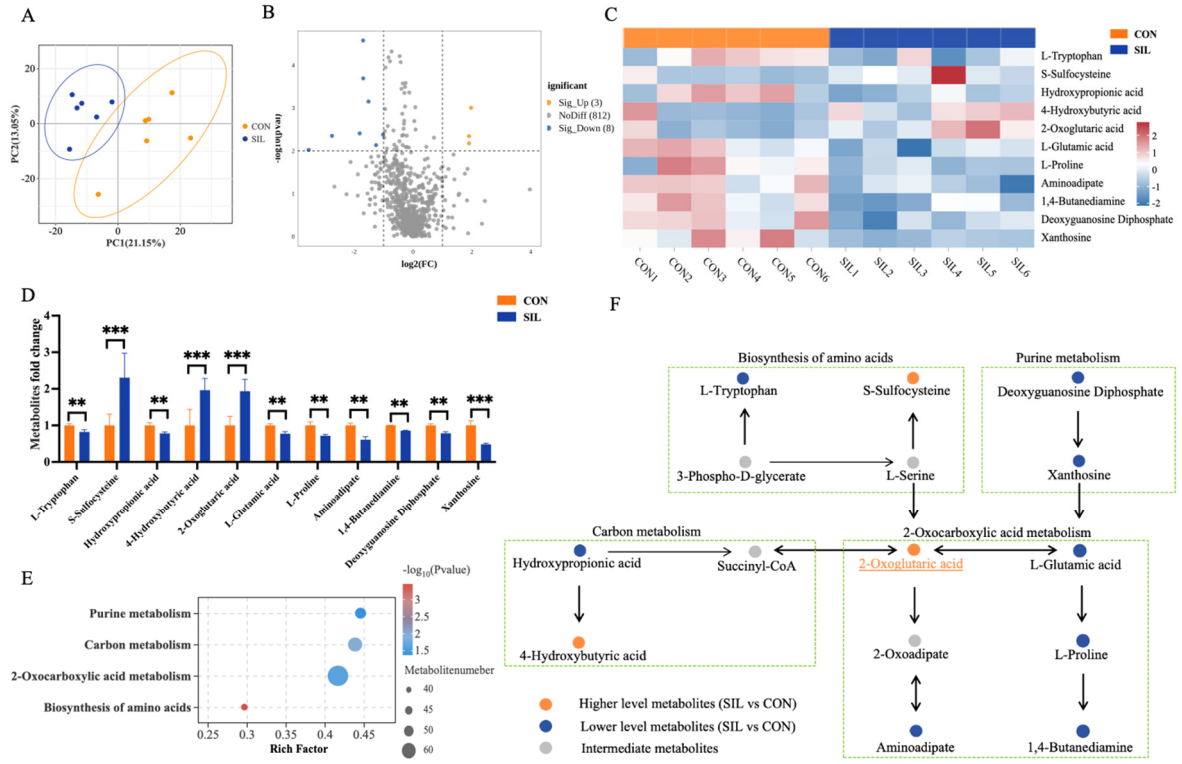

Figure 4. Effects of silymarin on plasma metabolites in heat stressed laying hens. **(A)** Principle component analysis score plot of two - group samples. **(B)** Volcano map of differentially regulated metabolites. **(C)** Differential metabolite heatmap. **(D)** Differential metabolite fold change bar graph. **(E)** Enriched metabolic pathways related network diagram. The *P* value is calculated by student t test and two-tailed. Data are presented as mean ± SEM, n=6. * $P<0.05$, ** $P<0.01$.

3.5. Silymarin Regulates Liver Lipid Metabolism

Three-dimensional PCA plot showed a clear separation between the two liver groups (Figure 5A). The volcano plot, applying $P < 0.05$ and $|FC| > 2$, uncovered 352 up-regulated and 483 down-regulated genes (Figure 5B). Functional enrichment highlighted Steroid biosynthesis, PPAR signalling and Fatty-acid biosynthesis as the top three affected pathways (Figure 5C). Protein–protein interaction analysis positioned FASN as the central hub, most tightly linked to PPAR-related genes (Figure 5D). Six up-regulated genes mapped to PPAR signalling, while two down-regulated genes

 doi:10.20944/preprints202602.1852.v1

belonged to Fatty-acid biosynthesis (Figure 5E). qPCR confirmed the expression trends for all but ACAA1 (Figure 5F). These data indicate that silymarin activates PPAR signalling and represses fatty-acid biosynthesis in heat-stressed layers.

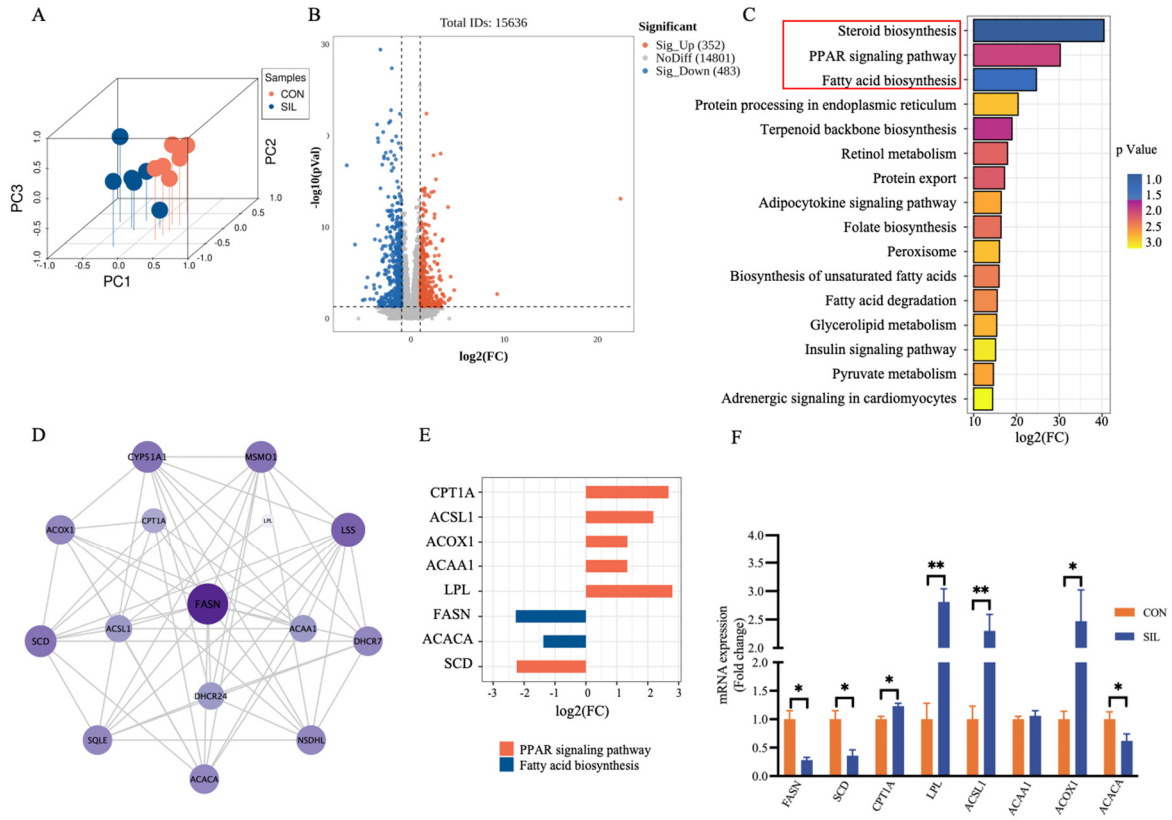

Figure 5. Hepatic transcriptomics. **(A)** 3D Principal component analysis (PCA) score plot of two - group samples. **(B)** Volcano plot of differentially expressed genes. **(C)** The top 16 significantly enriched KEGG pathways. **(D)** Protein-protein interaction (PPI) network of the differentially expressed genes in top 3 pathways. **(E)** Bar chart of key genes fold change. **(F)** qPCR to verify the expression of differential genes. The *P* value is calculated by student t test and two-tailed. Data are presented as mean ± SEM, n=6. * $P<0.05$, ** $P<0.01$.

3.6. Silymarin Suppresses Hepatic De Novo Lipogenesis and Promotes Fatty Acid β-Oxidation

A concise diagram summarizes the lipid metabolism regulatory network involved in the key genes regulated by silymarin (Figure 6A). 2D and 3D structural diagrams of silymarin (Figure 6B), followed by snapshots of its docked results within the catalytic pockets of SCD, ACOX1, ACSL1, FASN, CPT1A, LPL and ACACA (Figure 6C-I). Among these interactions, CPT1A produced the lowest binding energy (Table 1), indicating that the predicted complex with silymarin was the most stable. Among the core targets, Western blot confirmed that ACACA, FASN, CPT1A and ACSL1 changed in line with qPCR data, underscoring their pivotal role (Figure 6J). These dual effects converge to suppress de novo lipogenesis and accelerate fatty-acid β-oxidation, thereby restoring hepatic lipid balance.

Table 1. Protein-ligand molecular interaction results.

Protein name	Binding energy (kcal/mol)	Residues	Distance(Å)
CPT1A	-9.7	Glu676, Trp682, Ser259	2.57
ACSL1	-8.0	Ser593, Arg683	3.23
ACACA	-8.8	His211, Asn126, Ile128, Asp554	2.96

 doi:10.20944/preprints202602.1852.v1

FASN	-8.7	Arg1881, Arg1107, Arg1542	3.06
SCD	-8.0	Tyr529	3.00
LPL	-8.5	Gln60, Phe41, Glu38	2.90
ACOX1	-8.4	Asp615, Arg97, Asp410, Lys639	2.72

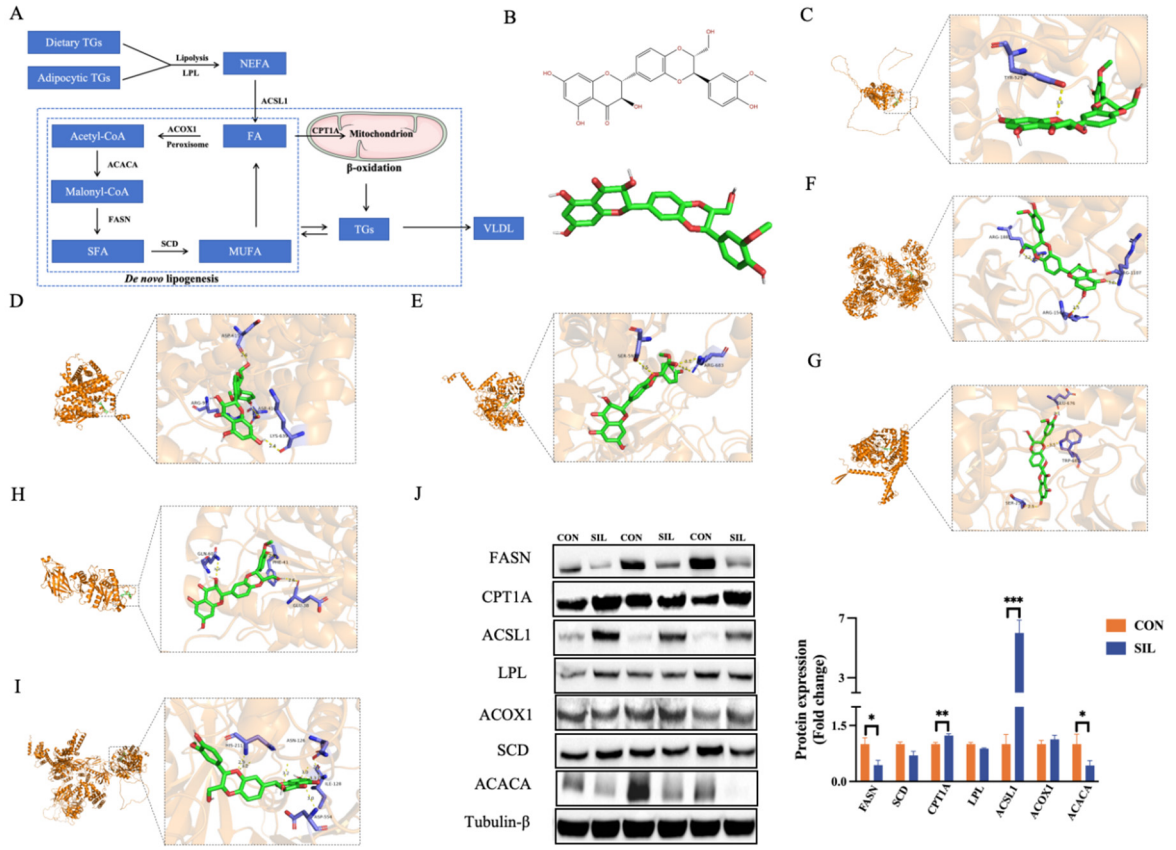

Figure 6. Analysis and verification of critical regulatory targets. **(A)** Schematic diagram of the regulatory mechanism of silymarin on liver lipid metabolism. **(B)** 2D and 3D structural diagrams of silymarin. **(C-I)** Molecular docking diagram of silymarin and core targets. **(K)** Western blot analysis of the differentially expressed proteins. The *P* value is calculated by student t test and two-tailed. Data are presented as mean ± SEM, n=6. * $P<0.05$, ** $P<0.01$.

3.7. Correlation Analysis

Correlation heat maps revealed tight links between key metabolites and proteins: 4-hydroxybutyric acid, 2-oxoglutaric acid and xanthosine emerged as the most influential (Figure 7A). Nonlinear regression analysis revealed a strong correlation between 2-oxoglutaric acid and FASN, with a high model fit (Figure 7B). Similarly, xanthine, 4-hydroxybutyric acid and ACACA showed strong correlations with high model fit (Figure 7I and M). Liver antioxidant indicators T-SOD, GSH, GSH Px have a strong positive correlation with 4-hydroxybutyric acid, 2-oxoglutaric acid, CPT1A, ACSL1, but a strong negative correlation with xanthine, ACACA, and FASN, egg weight and plasma HDL-C also have the same correlation, while MDA, ALT, and liver steatosis show the opposite trend (Figure 7N). Laying rate is significantly positively correlated with key metabolites 4-hydroxybutyric acid and 2-oxoglutaric acid, and significantly negatively correlated with xanthine, significantly positively correlated with core targets CPT1A and ACSL1, and significantly negatively correlated with ACACA and FASN (Figure 8A-B). Integrative pathway analysis revealed that elevated plasma levels of 4-hydroxybutyric acid and 2-oxoglutaric acid were associated with enhanced fatty acid β-oxidation and concurrent suppression of lipogenesis, whereas xanthosine exhibited an opposing

 doi:10.20944/preprints202602.1852.v1

regulatory influence on these metabolic pathways. Hepatic TG is significantly negatively correlated with key metabolites 4-hydroxybutyric acid and 2-oxoglutaric acid, and significantly positively correlated with xanthine, core targets CPT1A and ACSL1, and ACACA and FASN (Figure 8A-B).

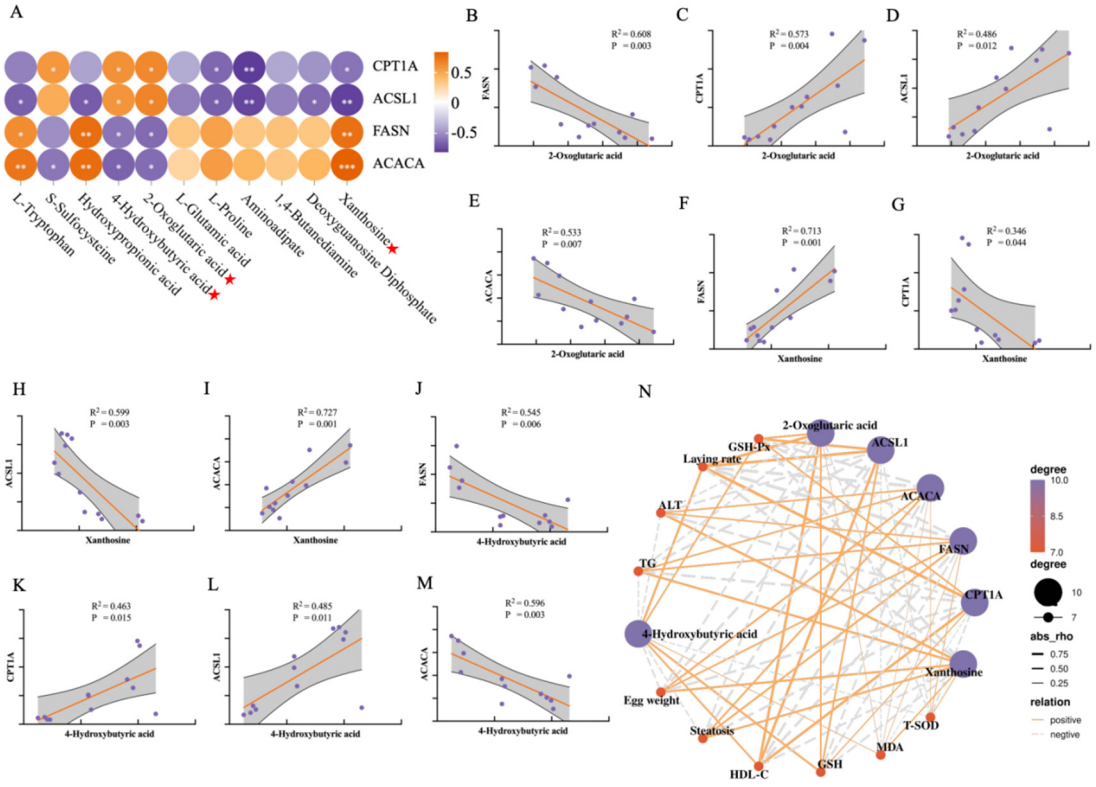

Figure 7. Correlation and nonlinear regression analysis between key metabolites and key proteins. **(A)** Correlation heatmap between differential metabolites and key proteins. **(B)** Nonlinear Regression Analysis 2-Oxoglutaric acid and FASN, **(C)** and CPT1A, **(D)** and ACSL1, **(E)** ACACA. **(F)** Nonlinear Regression Analysis Xanthosine and FASN, **(G)** and CPT1A, **(H)** and ACSL1, **(I)** ACACA. **(J)** Nonlinear Regression Analysis 4-Hydroxybutyric acid and FASN, **(K)** and CPT1A, **(L)** and ACSL1, **(M)** ACACA. **(N)** Correlation between regulatory targets of silymarin. The *P* value is calculated by student t test and two-tailed. Data are presented as mean ± SEM, n=6. * $P<0.05$, ** $P<0.01$, *** $P<0.001$.

 doi:10.20944/preprints202602.1852.v1

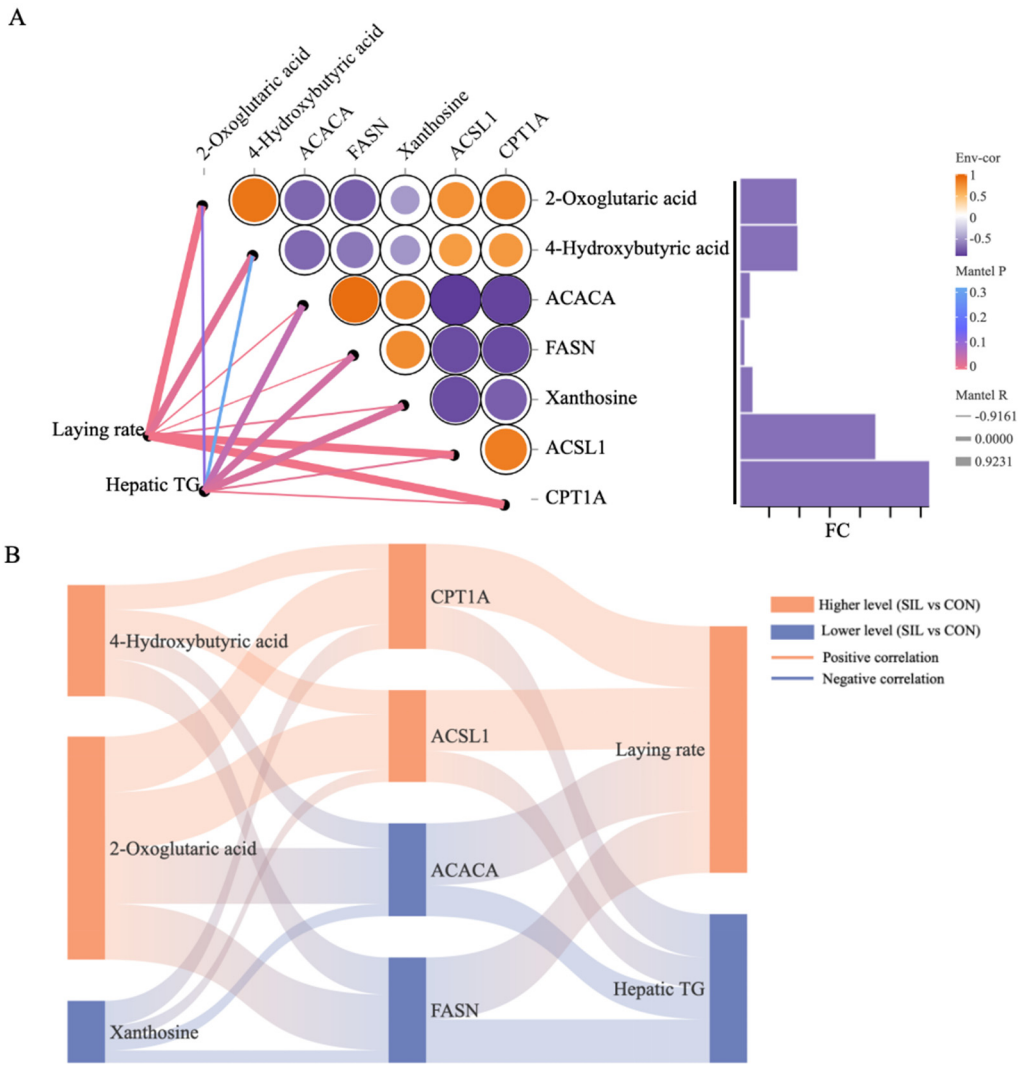

Figure 8. Correlation analysis. **(A)** Heat map of correlation between key differential proteins, key differential metabolites and apparent indicators. **(B)** Sankey diagram of key differential proteins, key differential metabolites and apparent indicators. n=6.

4. Discussion

This study provides a comprehensive exploration of the effects of dietary silymarin on heat-stressed laying hens through an integrative multi-omics approach. The findings demonstrate that silymarin at 100 mg/kg can significantly counteract the detrimental impacts of heat stress on liver health and egg production performance. By employing a multi-faceted research strategy that combines transcriptomic, metabolomic, and functional analyses, we have unveiled the molecular mechanisms through which silymarin ameliorates hepatic lipid metabolism and oxidative stress. This work advances our understanding of the role of natural bioactive compounds in mitigating the adverse effects of climatic stressors on livestock productivity. The results not only validate silymarin as a promising feed additive but also offer valuable insights for the development of targeted nutritional interventions in the poultry industry. The potential for silymarin to serve as a cornerstone in sustainable and resilient poultry production strategies amid escalating global temperatures underscores the significance of this research. Future studies could further explore the long-term effects of silymarin supplementation, its interactions with other nutrients, and its applicability across different poultry species and production systems.

Heat stress exerts multifaceted detrimental effects on laying hens, significantly impairing their production performance, egg quality, and physiological homeostasis. Chronic heat stress has been

 doi:10.20944/preprints202602.1852.v1

consistently shown to reduce egg production rate, egg weight, and eggshell quality, primarily due to decreased feed intake and disrupted nutrient metabolism [17,18]. Notably, silymarin linearly improved laying rate, egg weight, and feed conversion ratio (FCR) at doses of 0.02 ~ 0.06% [19]. From a practical standpoint, the observed dose-dependent effects of silymarin (0.02 ~ 0.06%) on laying performance and egg quality highlight its potential as an economically viable feed additive for mitigating HS-induced losses in poultry production. However, further studies are needed to evaluate its stability under extreme environmental conditions and its efficacy in other livestock species. The decline in eggshell strength and thickness under heat stress is attributed to metabolic alkalosis caused by panting, which reduces blood bicarbonate availability for shell mineralization [20]. In this study, egg quality such as haugh unit, albumen height, and yolk color were enhanced, due to the antioxidant properties of silymarin, it stabilizes the homeostasis of laying hens, reduces inflammation, and improves metabolism in the body [21,22].

Additionally, heat stress disrupts plasma biochemical parameters, including elevated creatinine and reduced albumin levels, indicating renal dysfunction [20], as well as increased triglycerides and cholesterol due to altered lipid metabolism [22]. Liver health is particularly compromised, with heat stress inducing oxidative damage, mitochondrial dysfunction, and hepatic lipid accumulation, leading to fatty liver syndrome [18,23]. However, in this study, silymarin reversed this situation, plasma biochemical analyses revealed reduced cholesterol and TG levels, alongside lowered NAS score and ALT activities, indicating improved lipid metabolism and hepatoprotection.

Heat stress induces oxidative damage and lipid peroxidation, leading to elevated serum ALT, AST, and cholesterol levels, however, silymarin reversed this situation in our work, and counteracted these effects by reducing MDA and enhancing SOD and GSH-Px activities, thereby preserving hepatic function [24]. And the key metabolites in the plasma metabolome reshaped by silymarin are closely related to antioxidant capacity. A pivotal observation herein is the silymarin-elicited augmentation of 2-oxoglutarate (α-KG), a central TCA-cycle intermediary pivotal to mitochondrial bioenergetics. A-KG enhances antioxidant defenses by upregulating GSH levels and reducing reactive oxygen species (ROS) accumulation [25,26]. In this study, these effects are further supported by silymarin-induced activation of antioxidant enzymes such as SOD and GSH-Px, suggesting a dual mechanism for mitigating oxidative stress. A-KG enhances mitochondrial fatty acid oxidation through two distinct mechanisms. First, α-KG activates AMP-activated protein kinase (AMPK) in hepatocytes, initiating downstream signaling that increases the phosphorylation of ACC. This phosphorylation inhibits ACC activity, reducing malonyl-CoA levels and subsequently relieving the inhibition of carnitine palmitoyltransferase 1 (CPT1) [27,28]. Second, α-KG serves as a substrate for the mitochondrial enzyme glutamate dehydrogenase (GDH), generating NADH that fuels the electron transport chain and improves oxidative phosphorylation efficiency [29]. This dual action creates a metabolic shift favoring lipid catabolism over storage. Silymarin enhances α-KG levels primarily by stimulating the tricarboxylic acid (TCA) cycle and mitochondrial metabolism. 4-hydroxybutyric (GHB) inhibits lipid synthesis and CO_2 production in mitochondria-containing tissues, including liver, this inhibition likely stems from GHB's interference with acetyl-CoA metabolism, a critical substrate for fatty acid synthesis, or its indirect suppression of mitochondrial respiration [30]. Silymarin's antioxidant properties reduce oxidative degradation of GHB, thereby stabilizing its plasma concentration [31,32]. Xanthosine (XTS), a purine nucleoside, modulates lipid metabolism through PPAR signaling, enhancing fatty acid uptake and utilization [33]. The mechanistic interplay between xanthosine's antioxidant and lipid-modulating properties appears centered on its ability to regulate mitochondrial function by maintaining mitochondrial membrane potential and enhancing oxidative phosphorylation capacity, xanthosine preserves cellular energy homeostasis while minimizing ROS generation [34]. This mitochondrial stabilization, potentially linked with GPX4 upregulation [35], contribute to reducing ferroptosis-induced hepatocyte damage, although further validation is required. However, the reduction in plasma xanthosine reflect enhanced hepatic uptake and intracellular metabolism of xanthosine, leading to its accelerated conversion into bioactive derivatives in the liver. Xanthosine is metabolized by purine nucleoside

 doi:10.20944/preprints202602.1852.v1

phosphorylase (PNP) to generate xanthine, which is further processed into uric acid - a potent antioxidant at physiological levels [36,37]. Silymarin enhances XTS levels by inhibiting xanthine oxidase (XO), an enzyme that degrades XTS into xanthine and uric acid [37].

Unlike previous studies primarily focusing on silymarin's antioxidant properties, our research reveals a novel, multi-target mechanism in which silymarin simultaneously modulates key lipogenic and oxidative pathways (ACACA, FASN, CPT1A, and ACSL1). The integration of plasma metabolomics and liver transcriptomics provides unprecedented insights into the dynamic interactions between lipid metabolism and antioxidant defenses. At the molecular level, we observed that silymarin significantly downregulated ACACA expression, consistent with the findings of Xie et al [37]. This inhibition reduces malonyl-CoA production, which serves dual roles: (1) as a substrate for fatty acid elongation and (2) as an allosteric inhibitor of CPT1A [38]. Our findings reveal that Silymarin downregulates key lipogenic genes, including ACACA and FASN, thereby reducing malonyl-CoA production and limiting long-chain fatty acid synthesis. Additionally, the upregulation of CPT1A and ACSL1 promotes mitochondrial fatty acid oxidation. Molecular docking results further confirm that silymarin binds to the regulatory domains of these enzymes, suggesting a direct modulatory effect on lipid metabolic pathways [39]. These effects are mediated through silymarin's inhibition of SREBP-1 nuclear translocation and transcriptional activity [40]. Our data revealed that silymarin treatment markedly upregulated CPT1A expression, facilitating mitochondrial fatty acid β-oxidation. This effect appears to be mediated through PPARα activation, as evidenced by increased PPARα binding to the CPT1A promoter region [41]. Furthermore, we identified ACSL1 as another key target of silymarin, with treatment significantly enhancing ACSL1 protein levels. This finding corroborates the work of Zhou et al [42], demonstrated that ACSL1 activation promotes fatty acid channeling toward oxidative pathways rather than esterification. The coordinated regulation of these four key targets (ACACA, FASN, CPT1A, and ACSL1) by silymarin creates a metabolic shift in hepatocytes from lipid accumulation to lipid utilization. This multi-target mechanism explains the compound's efficacy in ameliorating hepatic steatosis in NAFLD models [43]. The concurrent repression of lipogenesis and augmentation of β-oxidative capacity positions silymarin in a distinctive therapeutic niche compared with extant interventions that conventionally address only a singular facet.

Despite the mechanistic insight provided, the study is constrained by a single-dose design (100 mg/kg), which precludes establishing a dose-response curve or identifying the minimal effective concentration. Additionally, the 8-week controlled trial offers no evidence on the persistence of benefits under prolonged or cyclic heat-stress. Finally, data were generated in climate chambers with constant temperature - humidity indices; fluctuating ambient conditions, concurrent pathogens and variable feed intake, all of which may modulate silymarin efficacy. Multi-dose (50-200 mg/kg), long-term and on-farm studies are therefore warranted before commercial extrapolation.

5. Conclusion

In summary, dietary silymarin (100 mg/kg) mitigates heat-stress-induced hepatic lipid disruption and performance declines in laying hens. In a 8-week trial (THI > 73), silymarin increased laying rate, egg quality, enhanced antioxidant capacity and reduced hepatic steatosis, lowering triglyceride and cholesterol levels. Multi-omics revealed 11 plasma metabolites (e.g., 2-oxoglutaric acid) linked to purine metabolism and 835 hepatic genes affecting PPAR signaling and fatty acid biosynthesis. Silymarin suppressed lipogenesis (downregulating ACACA, FASN) and promoted β-oxidation (upregulating CPT1A, ACSL1), confirmed by molecular docking and Western blotting. Silymarin is a promising antioxidant feed additive to alleviate heat stress and enhance poultry productivity.

Supplementary Materials: The following supporting information can be downloaded at the website of this paper posted on Preprints.org.

 doi:10.20944/preprints202602.1852.v1

Author Contributions: J.G.: Writing-original draft, Methodology, Formal analysis, Data curation; H.R. and X.W.: Methodology, Formal analysis. C.Z.: Methodology. B.H.: Conceptualization. W.M.: Writing-review & editing, Validation, Supervision, Project administration, Funding acquisition, Conceptualization.

Funding: This work was supported by Grants from National Key Research and Development Program of China (No.2023YFD1300802).

Ethics approval and consent to participate: The animal experiments were approved by the Institutional Animal Care and Use Committee of Nanjing Agricultural University according to the Guidelines on Ethical Treatment of Experimental Animals (2006) No. 398 set by the Ministry of Science and Technology (2006, Beijing, China) (NJAULLSC2024062).

Data Availability Statement: All data generated or analyzed during this study are included in the manuscript. For any additional information or requests, please contact the corresponding author.

Conflicts of Interest: All authors declare that they have no conflicts of interest.

References

1. He, X.; Lu, Z.; Ma, B.; Zhang, L.; Li, J.; Jiang, Y.; Zhou, G.; Gao, F. Chronic heat stress damages small intestinal epithelium cells associated with the adenosine 5'-monophosphate-activated protein kinase pathway in broilers. *J. Agric. Food Chem.* **2018**, 66, 7301–7309.
2. Mangan, M.; Siwek, M. Strategies to combat heat stress in poultry production-A review. *J. Anim. Physiol. Anim. Nutr.* **2024**, 108, 576–595.
3. Li, G.M.; Liu, L.P.; Yin, B.; Liu, Y.Y.; Dong, W.W.; Gong, S.; Zhang, J.; Tan, J.H. Heat stress decreases egg production of laying hens by inducing apoptosis of follicular cells via activating the FasL/Fas and TNF-α systems. *Poult. Sci.* **2020**, 99, 6084–6093.
4. Ma, B.; Xing, T.; Li, J.; Zhang, L.; Jiang, Y.; Gao, F. Chronic heat stress causes liver damage via endoplasmic reticulum stress-induced apoptosis in broilers. *Poult. Sci.* **2022**, 101, 102063.
5. Tesakul, S.; Mitsuwan, W.; Morita, Y.; Kitpipit, W. Effects of heat stress on egg performance in laying hens under hot and humid conditions. *Vet. World* **2025**, 18, 851–858.
6. Gao, J.; Ren, H.; Wu, X.; Zou, C.; He, B.; Ma, W. Dietary glycerol monolaurate mitigates heat stress-induced disruption of intestinal homeostasis and hepatic lipid metabolism in laying hens. *Stress Biol.* **2025**, 5, 49.
7. Abdel-Moneim, A.E.; Shehata, A.M.; Khidr, R.E.; Paswan, V.K.; Ibrahim, N.S.; El-Ghoul, A.A.; Aldhumri, S.A.; Gabr, S.A.; Mesalam, N.M.; Elbaz, A.M.; Elsayed, M.A.; Wakwak, M.M.; Ebeid, T.A. Nutritional manipulation to combat heat stress in poultry - A comprehensive review. *J. Therm. Biol.* **2021**, 98, 102915.
8. Nanto-Hara, F.; Ohtsu, H. In laying hens, chronic heat stress-induced renal fibrosis is potentially promoted by indoxyl sulfate. *Sci. Rep.* **2024**, 14, 23213.
9. Yin, C.; Zhou, C.; Shi, Y.; Ge, Y.; Gao, X.; Wu, C.; Xu, Z.; Huang, C.; Hu, G.; Liu, P.; et al. Effects and potential mechanism of dietary vitamin C supplementation on hepatic lipid metabolism in growing laying hens under chronic heat stress. *J. Anim. Sci.* **2023**, 101, skad308.
10. Shakeri, M.; Oskoueian, E.; Le, H.H.; Shakeri, M. Strategies to combat heat stress in broiler chickens: Unveiling the roles of selenium, vitamin E and vitamin C. *Vet. Sci.* **2020**, 7, 71.
11. Zhao, Y.; Zhuang, Y.; Shi, Y.; Xu, Z.; Zhou, C.; Guo, L.; Liu, P.; Wu, C.; Hu, R.; Hu, G.; et al. Effects of N-acetyl-l-cysteine on heat stress-induced oxidative stress and inflammation in the hypothalamus of hens. *J. Therm. Biol.* **2021**, 98, 102927.
12. Gillessen, A.; Schmidt, H.H. Silymarin as supportive treatment in liver diseases: A narrative review. *Adv. Ther.* **2020**, 37, 1279–1301.
13. Lima, R.L.S.; Menegatto, M.B.D.S.; Almeida, L.T.; Magalhães, J.C.; Ferraz, A.C.; Magalhães, C.L.B. Silymarin exerts antioxidant and antiviral effects on Zika virus infection. *J. Virol. Methods* **2025**, 335, 115133.
14. Stephen-Robert, J.M.; Peddha, M.S.; Srivastava, A.K. Effect of silymarin and quercetin in a miniaturized scaffold in Wistar rats against non-alcoholic fatty liver disease. *ACS Omega* **2021**, 6, 20735–20745.

 doi:10.20944/preprints202602.1852.v1

15. Guo, Y.; Xu, Y.; Wang, D.; Yang, S.; Song, Z.; Li, R.; He, X. Dietary silymarin improves performance by altering hepatic lipid metabolism and cecal microbiota function and its metabolites in late laying hens. *J. Anim. Sci. Biotechnol.* **2024**, 15, 100.
16. Faryadi, S.; Sheikhahmadi, A.; Farhadi, A.; Nourbakhsh, H. Evaluating the therapeutic effect of different forms of silymarin on liver status and expression of some genes involved in fat metabolism, antioxidants and anti-inflammatory in older laying hens. *Vet. Med. Sci*. **2024**, 10, e70025.
17. Gholizadeh, H.; Torki, M.; Mohammadi, H. Production performance, egg quality and some blood parameters of heat-stressed laying hens as affected by dietary supplemental Vit B6, Mg and Zn. *Vet. Med. Sci.* **2022**, 8, 681–694.
18. Cornescu, G.M.; Panaite, T.D.; Untea, A.E.; Varzaru, I.; Saracila, M.; Dumitru, M.; Vlaicu, P.A.; Gavris, T. Mitigation of heat stress effects on laying hens' performances, egg quality, and some blood parameters by adding dietary zinc-enriched yeasts, parsley, and their combination. *Front. Vet. Sci*. **2023**, 10, 1202058.
19. Khan, S.U.; Jeon, Y.H.; Kim, I.H. Dietary inclusion of micelle silymarin enhances egg production, quality, and lowers blood cholesterol in Hy-line brown laying hens. *J. Anim. Physiol. Anim. Nutr*. **2024**, 108, 1038–1045.
20. Nanto-Hara, F.; Yamazaki, M.; Murakami, H.; Ohtsu, H. Chronic heat stress induces renal fibrosis and mitochondrial dysfunction in laying hens. *J. Anim. Sci. Biotechnol*. **2023**, 14, 81.
21. Sahin, E.; Bagci, R.; Bektur Aykanat, N.E.; Kacar, S.; Sahinturk, V. Silymarin attenuated nonalcoholic fatty liver disease through the regulation of endoplasmic reticulum stress proteins GRP78 and XBP-1 in mice. *J. Food Biochem*. **2020**, 44, e13194.
22. Gholamalian, R.; Mahdavi, A.H.; Riasi, A. Hepatic fatty acids profile, oxidative stability and egg quality traits ameliorated by supplementation of alternative lipid sources and milk thistle meal. *J. Anim. Physiol. Anim. Nutr.* **2022**, 106, 860–871.
23. Abulikemu, A.; Zhao, X.; Xu, H.; Li, Y.; Ma, R.; Yao, Q.; Wang, J.; Sun, Z.; Li, Y.; Guo, C. Silica nanoparticles aggravated the metabolic associated fatty liver disease through disturbed amino acid and lipid metabolisms-mediated oxidative stress. *Redox Biol*. **2023**, 59, 102569.
24. García-Muñoz, A.M.; Victoria-Montesinos, D.; Ballester, P.; Cerdá, B.; Zafrilla, P. A descriptive review of the antioxidant effects and mechanisms of action of berberine and silymarin. *Molecules* **2024**, 29, 4576.
25. He, R.; Wei, Y.; Peng, Z.; Yang, J.; Zhou, Z.; Li, A.; Wu, Y.; Wang, M.; Li, X.; Zhao, D.; Liu, Z.; Dong, H.; Leng, X. α-Ketoglutarate alleviates osteoarthritis by inhibiting ferroptosis via the ETV4/SLC7A11/GPX4 signaling pathway. *Cell Mol. Biol. Lett.* **2024**, 29, 88.
26. Liu, L.; Zhang, W.; Liu, T.; Tan, Y.; Chen, C.; Zhao, J.; Geng, H.; Ma, C. The physiological metabolite α-ketoglutarate ameliorates osteoarthritis by regulating mitophagy and oxidative stress. *Redox Biol*. **2023**, 62, 102663.
27. Cheng, D.; Zhang, M.; Zheng, Y.; Wang, M.; Gao, Y.; Wang, X.; Liu, X.; Lv, W.; Zeng, X.; Belosludtsev, K.N.; Su, J.; Zhao, L.; Liu, J. α-Ketoglutarate prevents hyperlipidemia-induced fatty liver mitochondrial dysfunction and oxidative stress by activating the AMPK-pgc-1α/Nrf2 pathway. *Redox Biol.* **2024**, 74, 103230.
28. Branco, R.C.S.; Camargo, R.L.; Batista, T.M.; Vettorazzi, J.F.; Lubaczeuski, C.; Bomfim, L.H.M.; Silveira, L.R.; Boschero, A.C.; Zoppi, C.C.; Carneiro, E.M. Protein malnutrition mitigates the effects of a high-fat diet on glucose homeostasis in mice. *J. Cell. Physiol.* **2019**, 234, 6313–6323.
29. Legendre, F.; Tharmalingam, S.; Bley, A.M.; MacLean, A.; Appanna, V.D. Metabolic adaptation and NADPH homeostasis evoked by a sulfur-deficient environment in Pseudomonas fluorescens. *Antonie Van Leeuwenhoek* **2020**, 113, 605–616.
30. Silva, A.R.; Ruschel, C.; Helegda, C.; Brusque, A.M.; Wannmacher, C.M.; Wajner, M.; Dustra-Filho, C.S. Inhibition of rat brain lipid synthesis in vitro by 4-hydroxybutyric acid. Metab. *Brain Dis*. **1999**, 14, 157–164.
31. Sgaravatti, A.M.; Magnusson, A.S.; Oliveira, A.S.; Mescka, C.P.; Zanin, F.; Sgarbi, M.B.; Pederzolli, C.D.; Wyse, A.T.; Wannmacher, C.M.; Wajner, M.; Dutra-Filho, C.S. Effects of 1,4-butanediol administration on oxidative stress in rat brain: study of the neurotoxicity of gamma-hydroxybutyric acid in vivo. *Metab. Brain Dis*. **2009**, 24, 271–282.

 doi:10.20944/preprints202602.1852.v1

32. Sgaravatti, A.M.; Sgarbi, M.B.; Testa, C.G.; Durigon, K.; Pederzolli, C.D.; Prestes, C.C.; Wyse, A.T.; Wannmacher, C.M.; Wajner, M.; Dutra-Filho, C.S. Gamma-hydroxybutyric acid induces oxidative stress in cerebral cortex of young rats. *Neurochem. Int*. **2007**, 50, 564–570.
33. Choudhary, R.K.; Choudhary, S.; Verma, R. In vivo response of xanthosine on mammary gene expression of lactating Beetal goat. *Mol. Biol. Rep*. **2018**, 45, 581–590.
34. Xu, Y.; Zhou, W.; Fan, Z.; Cheng, Y.; Xiao, Y.; Liu, Y.; Li, X.; Ji, Z.; Fan, Y.; Ma, G. Xanthosine alleviates myocardial ischemia-reperfusion injury through attenuation of cardiomyocyte ferroptosis. *Cell Mol. Biol. Lett*. **2025**, 30, 93.
35. Guo, Y.Y.; Liang, N.N.; Zhang, X.Y.; Ren, Y.H.; Wu, W.Z.; Liu, Z.B.; He, Y.Z.; Zhang, Y.H.; Huang, Y.C.; Zhang, T.; et al. Mitochondrial GPX4 acetylation is involved in cadmium-induced renal cell ferroptosis. *Redox Biol*. **2024**, 73, 103179.
36. Ahmed, S.A.; Sarma, P.; Barge, S.R.; Swargiary, D.; Devi, G.S.; Borah, J.C. Xanthosine, a purine glycoside mediates hepatic glucose homeostasis through inhibition of gluconeogenesis and activation of glycogenesis via regulating the AMPK/ FoxO1/AKT/GSK3β signaling cascade. *Chem. Biol. Interact.* **2023**, 371, 110347.
37. Xie, Z.; Ding, S.Q.; Shen, Y.F. Silibinin activates AMP-activated protein kinase to protect neuronal cells from oxygen and glucose deprivation-re-oxygenation. *Biochem. Biophys. Res. Commun*. **2014**, 454, 313–319.
38. Softic, S.; Meyer, J.G.; Wang, G.X.; Gupta, M.K.; Batista, T.M.; Lauritzen, H.P.M.M.; Fujisaka, S.; Serra, D.; Herrero, L.; Willoughby, J.; et al. Dietary sugars alter hepatic fatty acid oxidation via transcriptional and post-translational modifications of mitochondrial proteins. *Cell Metab*. **2019**, 30, 735–753.e4.
39. Maréchal, L.; Sicotte, B.; Caron, V.; Brochu, M.; Tremblay, A. Fetal cardiac lipid sensing triggers an early and sex-related metabolic energy switch in intrauterine growth restriction. *J. Clin. Endocrinol. Metab.* **2021**, 106, 3295–3311.
40. Hüttl, M.; Markova, I.; Miklankova, D.; Zapletalova, I.; Poruba, M.; Racova, Z.; Vecera, R.; Malinska, H. The beneficial additive effect of silymarin in metformin therapy of liver steatosis in a pre-diabetic model. *Pharmaceutics* **2021**, 14, 45.
41. Jiang, X.; Geng, H.; Zhang, C.; Zhu, Y.; Zhu, M.; Feng, D.; Wang, D.; Yao, J.; Deng, L. Circadian rhythm enhances mTORC1/AMPK pathway-mediated milk fat synthesis in dairy cows via the microbial metabolite acetic acid. *J. Agric. Food Chem*. **2024**, 72, 28178–28193.
42. Zhou, Y.; Li, Y.; Chen, G.; Guo, X.; Gao, X.; Meng, J.; Xu, Y.; Zhou, N.; Zhang, B.; Zhou, X. ACSL1-mediated fatty acid β-oxidation enhances metastasis and proliferation in endometrial cancer. *Front. Biosci.* **2024**, 29, 1247.
43. Jaffar, H.M.; Al-Asmari, F.; Khan, F.A.; Rahim, M.A.; Zongo, E. Silymarin: Unveiling its pharmacological spectrum and therapeutic potential in liver diseases-A comprehensive narrative review. *Food Sci. Nutr.* **2024**, 12, 3097–3111.